NASA Technical Memorandum 107517 ARL–MR–363

NASA-TM-107517
19980206267

Experimental Performance of a Micromachined Heat Flux Sensor

S. Stefanescu
Case Western Reserve University, Cleveland, Ohio

R.G. DeAnna
U.S. Army Research Laboratory, Lewis Research Center, Cleveland, Ohio

M. Mehregany
Case Western Reserve University, Cleveland, Ohio

April 1998

The NASA STI Program Office . . . in Profile

Since its founding, NASA has been dedicated to the advancement of aeronautics and space science. The NASA Scientific and Technical Information (STI) Program Office plays a key part in helping NASA maintain this important role.

The NASA STI Program Office is operated by Langley Research Center, the Lead Center for NASA's scientific and technical information. The NASA STI Program Office provides access to the NASA STI Database, the largest collection of aeronautical and space science STI in the world. The Program Office is also NASA's institutional mechanism for disseminating the results of its research and development activities. These results are published by NASA in the NASA STI Report Series, which includes the following report types:

- TECHNICAL PUBLICATION. Reports of completed research or a major significant phase of research that present the results of NASA programs and include extensive data or theoretical analysis. Includes compilations of significant scientific and technical data and information deemed to be of continuing reference value. NASA's counterpart of peer-reviewed formal professional papers but has less stringent limitations on manuscript length and extent of graphic presentations.

- TECHNICAL MEMORANDUM. Scientific and technical findings that are preliminary or of specialized interest, e.g., quick release reports, working papers, and bibliographies that contain minimal annotation. Does not contain extensive analysis.

- CONTRACTOR REPORT. Scientific and technical findings by NASA-sponsored contractors and grantees.

- CONFERENCE PUBLICATION. Collected papers from scientific and technical conferences, symposia, seminars, or other meetings sponsored or cosponsored by NASA.

- SPECIAL PUBLICATION. Scientific, technical, or historical information from NASA programs, projects, and missions, often concerned with subjects having substantial public interest.

- TECHNICAL TRANSLATION. English-language translations of foreign scientific and technical material pertinent to NASA's mission.

Specialized services that complement the STI Program Office's diverse offerings include creating custom thesauri, building customized data bases, organizing and publishing research results . . . even providing videos.

For more information about the NASA STI Program Office, see the following:

- Access the NASA STI Program Home Page at ***http://www.sti.nasa.gov***

- E-mail your question via the Internet to help@sti.nasa.gov

- Fax your question to the NASA Access Help Desk at (301) 621-0134

- Telephone the NASA Access Help Desk at (301) 621-0390

- Write to:
  NASA Access Help Desk
  NASA Center for AeroSpace Information
  800 Elkridge Landing Road
  Linthicum Heights, MD 21090-2934

NASA Technical Memorandum 107517 ARL–MR–363

Experimental Performance of a Micromachined Heat Flux Sensor

S. Stefanescu
Case Western Reserve University, Cleveland, Ohio

R.G. DeAnna
U.S. Army Research Laboratory, Lewis Research Center, Cleveland, Ohio

M. Mehregany
Case Western Reserve University, Cleveland, Ohio

Prepared for the
Joint Propulsion Conference
cosponsored by AIAA, ASME, SAE, and ASEE
Seattle, Washington, July 6–9, 1997

National Aeronautics and
Space Administration

Lewis Research Center

April 1998

This report contains preliminary findings, subject to revision as analysis proceeds.

Available from

NASA Center for Aerospace Information
800 Elkridge Landing Road
Linthicum Heights, MD 21090-2934
Price Code: A03

National Technical Information Service
5287 Port Royal Road
Springfield, VA 22100
Price Code: A03

EXPERIMENTAL PERFORMANCE OF A MICROMACHINED HEAT FLUX SENSOR

S. Stefanescu, R. G. DeAnna* and M. Mehregany
Microfabrication Laboratory
Department of Electrical Engineering and Applied Physics
Case Western Reserve University
Cleveland, OH 44106

Abstract

Steady-state and frequency response calibration of a microfabricated heat-flux sensor have been completed. This sensor is batch fabricated using standard, micromachining techniques, allowing both miniaturization and the ability to create arrays of sensors and their corresponding interconnects. Both high-frequency and spatial response is desired, so the sensors are both thin and of small cross-sectional area. Thin-film, temperature-sensitive resistors are used as the active gauge elements. Two sensor configurations are investigated: a Wheatstone-bridge using four resistors; and a simple, two-resistor design. In each design, one resistor (or pair) is covered by a thin layer (5000 Å) thermal barrier; the other resistor (or pair) is covered by a thick (5 μm) thermal barrier. The active area of a single resistor is 360 μm by 360 μm; the total gauge area is 1.5 mm square. The resistors are made of 2000 Å-thick metal; and the entire gauge is fabricated on a 25 μm-thick flexible, polyimide substrate. Heat flux through the surface changes the temperature of the resistors and produces a corresponding change in resistance. Sensors were calibrated using two radiation heat sources: a furnace for steady-state, and a light and chopper for frequency response.

Introduction

Various thin-film or micromachined heat-flux sensors have been proposed[1-5]. These are all point-measurement devices which require installation of both the sensor and the interconnects for sensor power and signal output. This can be very costly and time consuming. Most of this installation can be avoided by integrating the sensors and interconnects in a single, batch-fabricated process. Installation becomes, essentially, a one-step process. Instead of bonding individual sensors and interconnects to the test hardware, only a single flex-circuit containing wires and sensors is required. A sensor package of this sort has been recently developed and fabricated by Advanced MicroMachines Incorporated[7]. This paper will discuss the calibration of a single sensor.

There are several thin-film sensor designs for measuring unsteady heat flux through a surface. These designs use either thermocouples or temperature-sensitive resistors separated by a thermal barrier. The temperature difference across the barrier is proportional to the heat flux. Typically, these thin-film gauges have sufficiently-low thermal mass for unsteady measurements[1]. In contrast, most conventionally-fabricated heat-flux gauges have long, thermal time constants with correspondingly poor high-frequency response, e.g., the plug-type sensor[6].

The thin-film sensor described in this paper uses temperature-sensitive resistors covered by a thermal barrier and is built on a flexible substrate using microfabrication techniques. The sensor was developed for low-temperature applications, e.g., shock-tunnel testing where temperatures remain below 300°C, and high-frequency measurements are necessary since the tunnel operates for only 20 to 25 msec. The thin-film resistors change temperature when heat flows normal to the surface. The

* Visiting scientist on leave from US Army Research Laboratory, NASA Lewis Research Center, Cleveland, Ohio 44106.

temperature variation causes a resistance change which is reflected in the output voltage. With unsteady heat flux, the bottom resistor has a smaller peak-to-peak amplitude than the top resistor. At high frequency, the signal propagation depth is such that only the top resistor's temperature varies with time. This behavior makes signal processing complicated and sensor calibration essential.

Sensor Design and Construction

A typical thin-film sensor layout is illustrated in Fig. 1. The sensor sensitivity is inversely proportional to the square root of the product of thermal conductivity, specific heat, and density of the thermal barrier. For high sensitivity, a low conductivity, density, and specific heat thermal-barrier substrate is desired. Polyimide was chosen as the most attractive substrate material. It has low conductivity, excellent thermal and mechanical properties up to 300°C, and a well-developed adhesive technology due to its wide use in strain gauges.

The material and design of the thin-film resistance thermometers must also be considered. For a resistor biased with a constant current, the temperature induced voltage change is

$$\delta V = \alpha V \delta T = \alpha I R \delta T, \tag{1}$$

where $V=IR$ represents the total voltage drop across the resistor. Thus, the sensitivity of the sensor is directly proportional to both its temperature coefficient and the excitation voltage. The excitation voltage is constrained by the Joule heating I^2R or dissipation in the film. This heat dissipation must be kept small compared to the heat flux being measured. The excitation voltage can be set by[1]

$$I = \sqrt{\frac{t}{\rho}} w \sqrt{Q_e}, \tag{2}$$

where Q_e is the heat flux dissipated in the film,

$$Q_e = \frac{I^2 R}{lw} = \frac{I^2 \rho}{t w^2}, \tag{3}$$

l and w are the film length and width, ρ is the volume resistivity, and t is the film thickness. Substituting into the expression for the gauge sensitivity gives

$$\frac{\delta V}{\delta T} = \sqrt{\frac{\rho}{t}} \alpha l \sqrt{Q_e}. \tag{4}$$

This implies that long, thin films with high-volume resistivity and temperature coefficient are most sensitive. The term $\alpha\sqrt{\rho}$ is only a function of the resistor material. It is $6.9 \cdot 10^{-3}$ $\sqrt{\mu\Omega \cdot \mathrm{cm}}/^{\circ}\mathrm{C}$ for aluminum; it is $8.8 \cdot 10^{-3}$ for copper, and, $27.8 \cdot 10^{-3}$ for platinum. Other factors influence the final choice of metal: surface temperature changes resulting from the thermal resistance and capacity of the film, adhesion of the film to the substrate, and residual stresses induced by the deposition process.

Once the substrate and resistor materials are selected, the thermal-barrier thickness is determined. If sensitivity alone is considered, then the thickest barrier which doesn't interfere with the flow should be used. However, a thick thermal barrier will have a large thermal time constant and poor frequency response. The thermal time constant is based on the thermal diffusivity of the material and the spacing between resistors as given by

$$\tau = \frac{\delta^2}{4\alpha}, \tag{5}$$

where δ is the barrier thickness and α the thermal diffusivity. Above a certain frequency, the signal doesn't propagate to the lower resistor. In this design, one resistor is covered by 5000 Å thick polyimide; the other is covered by 5.4 μm. This gives a frequency of 37.5 kHz, above which the bottom resistor remains at constant temperature.

The resistor layout is the final design parameter to consider. It is desirable to make the cross-sectional area of each resistor and the entire resistor combination as small as possible so that the sensor has high spatial resolution. They can't be made smaller than the minimum size dictated by the photolithography and batch processing fabrication techniques. And as shown in Eq. 4, the gauge sensitivity is proportional to the line length. Considering these restrictions, a single resistor was designed with 6 μm line widths, 6 μm spaces between lines and 360 μm by 360 μm in area for a design resistance of approximately 300 ohms.

One sensor configuration employed two pairs of resistors in a Wheatstone bridge as illustrated in

Fig. 2. Fig. 3 shows an enlarged plan view of a typical sensor. The resistor pairs are matched along the diagonal. The pair with the dark band around the perimeter is covered by the thin polyimide. The entire sensor area is approximately 1.5 mm by 1.5 mm. When a uniform heat flux is applied on the surface, a temperature gradient develops inside the thermal barrier layer according to Fourier's conduction law. The resistor pair buried under the thick barrier reaches T_2. The more exposed pair is at the higher temperature T_1. The four resistors are arranged in the bridge so that in the ideal case of a balanced bridge (zero output voltage with zero heat flux) the output voltage is proportional to the difference between T_1 and T_2. As will be discussed in the section on electrical theory, it wasn't possible to achieve balanced bridge in practice, since the bridge resistors were not trimmed subsequent to fabrication.. When the bridge isn't balanced, there's a temperature-dependent error term in the expression for heat flux. Therefore, a simpler design using only half the Wheatstone bridge was investigated. This sensor used only two resistors: one thick polyimide covered and one thin polyimide covered.

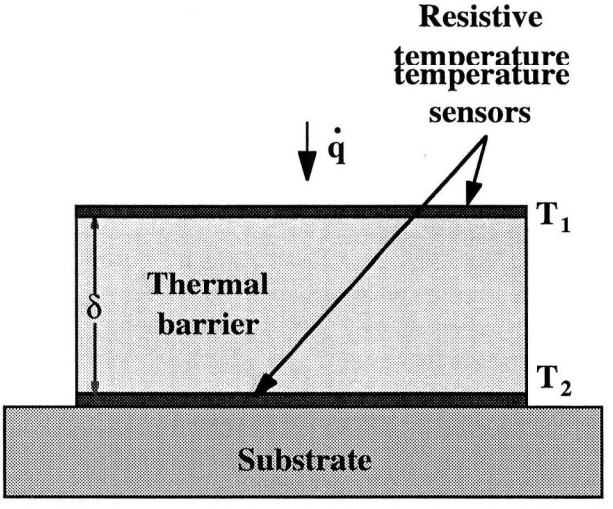

Figure 1. Sensor operating principle.

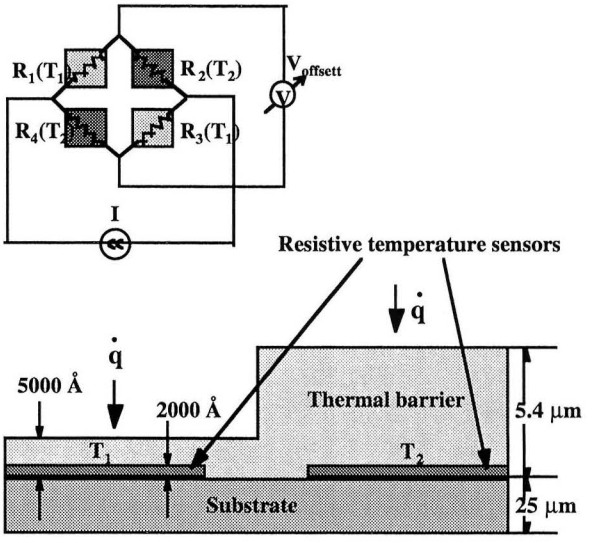

Figure 2. Wheatstone-bridge configuration and sensor cross-section.

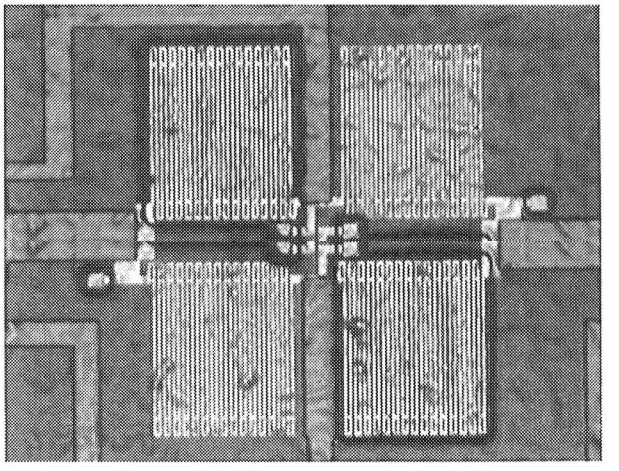

Figure 3. Top view of sensor.

Steady-State Calibration

The calibration was done in an ambient-temperature environment with a radiation heat-flux source. A reference sensor was used to determine the heat flux. To insure good heat transfer from the radiation source, the sensor was blackened with a marking pen. This coating had good opacity and low thermal inertia. Ideally, the black coating would have zero reflectivity so that all the incident radiation entered the gauge; it would also have zero transmissivity so that all the radiation which entered the gauge was converted to heat. In reality, the reflectivity is not zero - some of the incident radiation is reflected; and the transmissivity is not zero - some of the radiation

entering the sensor passes through the coating. Non-zero coating transmissivity allows some of the radiation to pass through the coating into the polyimide layer. This is a source of error since polyimide is transparent to light.

As shown in Fig. 4, a temperature-controlled furnace was used for steady-state calibration. Embedded in the furnace walls, is a helically-shaped, wire-coil heating element -- the radiation source. A thermocouple measures the air temperature in the hollow cylinder. The furnace has a 2.54 cm diameter opening at the bottom through which radiation escapes. To eliminate the room from the heat exchange and achieve a two-body, radiation problem, the furnace is placed as near the sensor surface as possible.

The reference gauge used during calibration was of plug-type design, as shown in Fig. 5 and described in reference[6]. This sensor uses three thermocouples welded to a central post which is surrounded by air. We assume constant heat flux along the length of the post,. Thus, the heat flux is proportional to the temperature difference between thermocouple junctions.

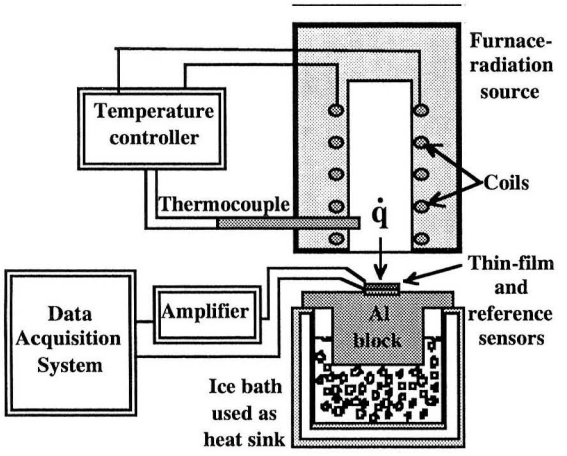

Figure 4. Steady-state calibration setup.

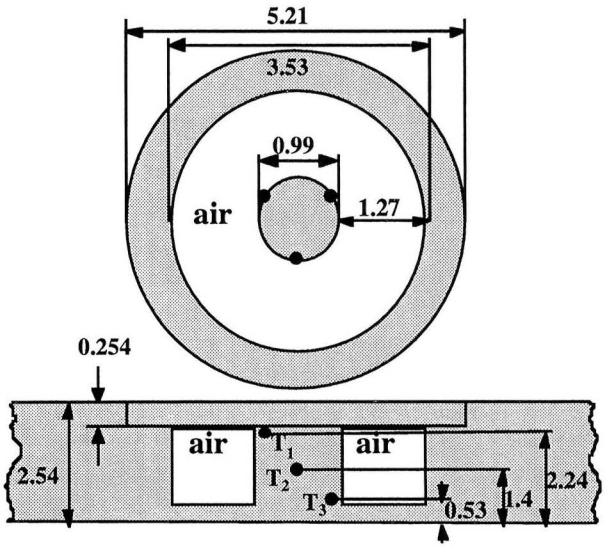

Figure 5. Plug-type, heat-flux sensor. All dimensions are in mm.

For calibration, both the thin-film and the reference sensors must be under identical heat flux. The easiest way to achieve this is to create a layered structure where both sensors are on the same unidirectional thermal flow path. The thin film sensor was bonded using thermally conductive epoxy to an aluminum plate of dimensions similar to the steel plate which holds the reference sensor. The aluminum plate holding the thin-film sensor was next mounted atop the reference sensor. This structure was attached to an aluminum block (Fig. 6), and the block was placed in an ice bath. Thermally conductive paste was applied between these metallic parts. The assembled structure was placed under the radiation source (Fig. 4). This layered configuration for the thin film and reference sensors was preferred to another configuration where the sensors weren't attached to each other. This second configuration required separate measurements of each sensor under the radiative source and was deemed to be less accurate than the layered approach. Also, the layered calibration setup avoids the requirement of coating both sensors with a material of the same emmissivity. This would be required for the separate-measurement configuration to insure identical heat flux for both sensors.

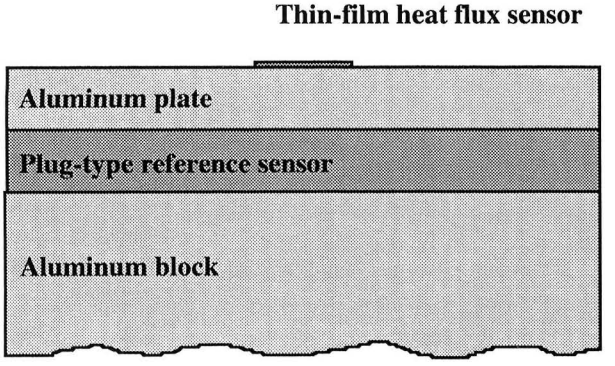

Figure 6. Layered structure containing sensor and reference gauge.

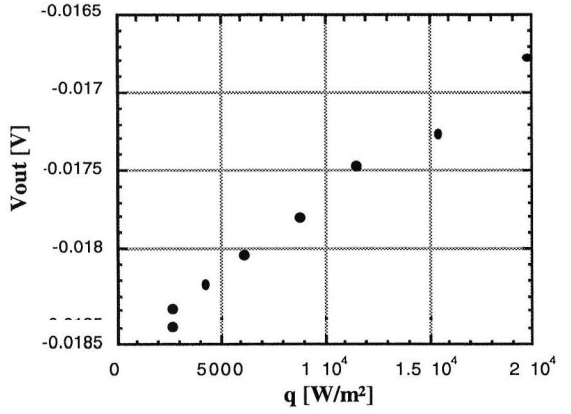

Figure 7. Thin-film sensor output voltage versus heat flux calculated by the reference gauge.

During calibration, the outputs of the two sensors were recorded simultaneously using a digital voltmeter and two digital thermometers connected by a IEEE488/GPIB bus to a computer. The thin-film sensor was operated using an external, DC, constant-current source of 0.6 mA. The output was amplified by a factor of ten by an off-sensor instrumentation amplifier. For the reference sensor, the thermocouple readings were referenced to 0°C using an ice bath in which the junctions between the thermocouple wires and the multimeter copper wires were immersed. The thin-film sensor output versus computed heat flux from the reference gauge is shown in Fig. 7.

Frequency Response

Frequency response calibration was done using a radiation source and a mechanical beam chopper. The first setup included a He-Ne laser source with power output of 20 mW and a wavelength of 633 nm. Because the beam diameter was of 0.7 mm, compared to a 1 mm^2 sensor, the entire sensor could not be under uniform heat flux. Beam expansion was attempted, but the energy density was too low for adequate output signal level. A microscope light source with a larger beam diameter was used instead. The sensor output was amplified and displayed in the frequency domain after performing an FFT. These data were used to generate Fig. 9.

As shown in Fig. 8, a mechanical chopper was placed between the light source and the sensor. The chopper produced a heat-flux which resembled the positive half of a sinusoidal wave.

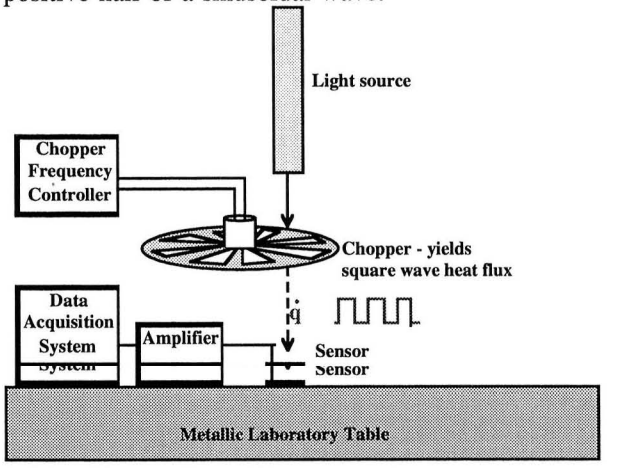

Figure 8. Frequency response calibration setup.

The mechanical chopper used a disk with 240 apertures. Chopping frequencies between 500 Hz and 8 KHz were generated. Plots of the bridge output voltage amplitude versus frequency are shown in Fig. 9. The graphs are normalized with respect to the amplitude at 500 Hz. The results show a decreasing amplitude with increasing frequency. Theory predicts that the amplitude of the temperature variation for each of the resistors decreases according to the inverse square-root of frequency. Hence, the sensor output voltage, which depends on temperature difference between resistors, should decay in a similar fashion. The experiments were limited to a 8 kHz chopping frequency; above this frequency, the signal was too small. Re0sults could be obtained at higher frequencies with a stronger energy source.

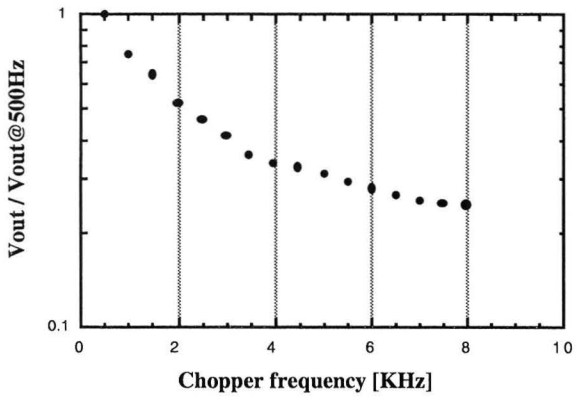

Figure 9. Normalized frequency response of the thin-film sensor.

Finite Element Analysis

Finite element analysis of the sensor frequency response was done using the ANSYS software package.

The model contained two resistors with different thicknesses of thermal barrier. Because the distance between two resistors was much larger than the sensor thickness, the horizontal heat flux is negligible with respect to the vertical and a 1-D model suffices. Although the two resistors are in the same model, they are thermally independent.

Each resistor model contains only two columns of elements in the horizontal direction. Adiabatic boundary conditions were applied on the sides of the model. These boundary conditions forced one-dimensional heat transfer and insured uniform heat flux at any given horizontal cross-section. In the vertical direction, each resistor model consists of a stack of four layers: on top, polyimide thermal barriers of 5 and 50 elements, for the thin and thick barriers, respectively; next, 2 aluminum elements for the resistor; then, 250 polyimide elements of 0.1 μm thickness representing the substrate; lastly, 200 elements of 0.4 μm thickness for the silicon backing. The total stack vertical dimension was 110 μm for the thick-coated model and 85 μm for the thin-coated model. We can estimate the lowest frequency where boundary conditions do not create problems using the expression for the thermal propagation depth, given by $\delta = 2\sqrt{\alpha / f}$. Using the overall model dimensions given above, this frequency is approximately 100 Hz. Below 100 Hz, the signal applied at the inlet boundary will be observed at the exit boundary. Well above 100 Hz, the exit boundary is not sensitive to the signal at the inlet boundary.

A square-wave, heat-flux boundary condition was applied at the inlet boundary, and a constant heat flux equal to the time averaged square wave was applied at the exit boundary. Below 100 Hz, the signal propagation depth is of the order of magnitude as the model length, and the constant-heat-flux exit condition fails. For all of the simulations, the temperature variation for the two resistors were recorded and plotted.

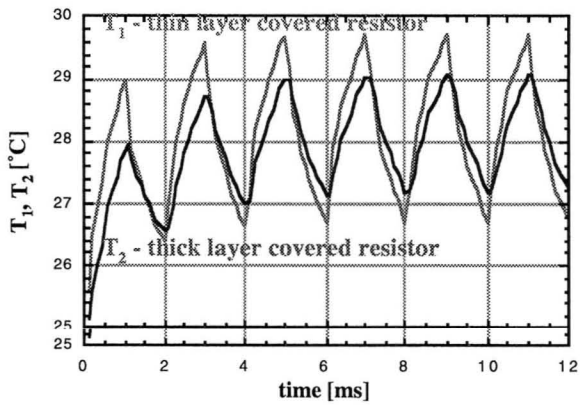

Figure 10. Temperature variations for the two resistors at 500 Hz.

At 500 Hz, the temperature variations of the two resistors and the temperature difference are shown in Figs. 10 and 11. As shown, the amplitude for the thick-covered resistor is smaller than that of the thin-covered resistor. Figure 12 gives the two temperatures at 20 kHz. The temperature variation for the top resistor decreases, while the thick-layer resistor amplitude variation has reached steady state.

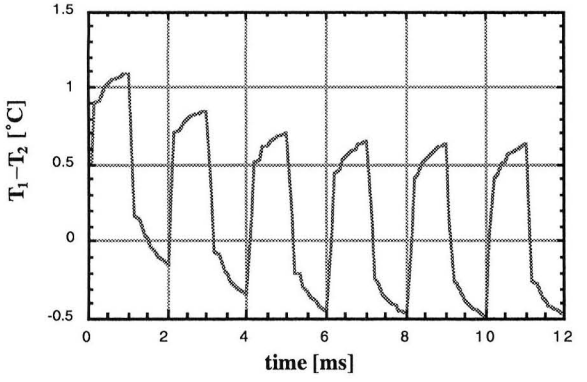

Figure 11. Temperature difference between the two resistors at 500 Hz.

Comparing Figs. 9 and 13, the experimental frequency response decays faster than the model predictions. This could be caused by either the light source or chopper characteristics which do not generate a true square wave.

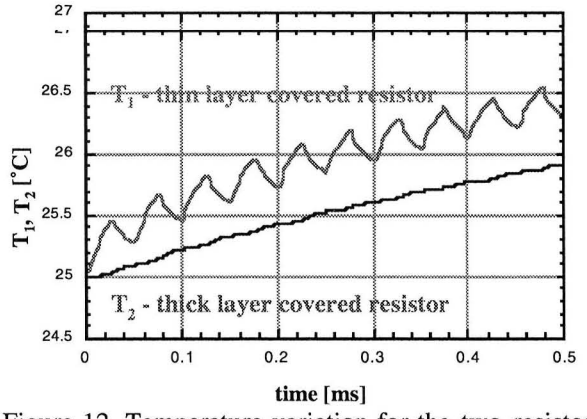

Figure 12. Temperature variation for the two resistors at 20 Khz.

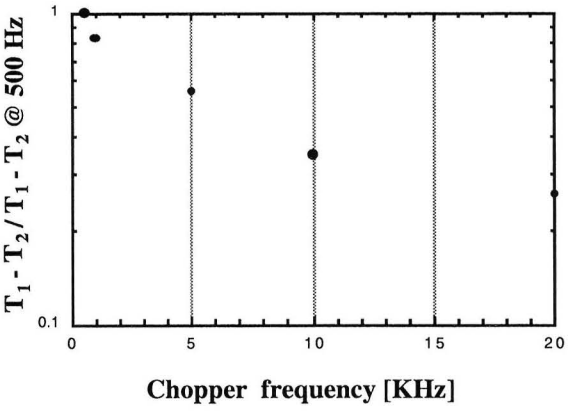

Figure 13. Finite Element Analysis frequency response.

Theoretical Electrical Behavior

Both the Wheatstone bridge and the two-resistor sensor's electrical behavior must be understood before accurate measurements are possible. In both sensor types, it is desirable to have identical resistors. This automatically ensures that the output voltage will be zero at zero heat flux. When the voltage will be zero at zero heat flux. When the resistors aren't equal, there is an offset voltage.

In certain applications, this resistance imbalance may be negligible, and the sensor operated without compensation. In other cases, this imbalance causes an error of the same order of magnitude as the signal due to heat flux. As compensation, a balance resistor is often used with Wheatstone bridges; however, for heat transfer measurements, a balance resistor isn't effective, because there's always a temperature difference between it and the sensor resistors.
Consider the operation of a Wheatstone-bridge. with both current and voltage biasing. For current bias, the output voltage is

$$V_{out} = I\frac{R_2R_4 - R_1R_3}{R_1 + R_2 + R_3 + R_4}. \qquad (6)$$

In voltage bias, the output voltage is

$$V_{out} = V\frac{R_2R_4 - R_1R_3}{(R_1 + R_2)(R_3 + R_4)}. \qquad (7)$$

I and V represent the constant current or voltage and the R_i's are the resistances of the individual resistors,

which are sensitive to both ambient temperature and heat flux. Define R_{i0} as the resistances at the reference temperature T_0. Ideally, the R_{i0}'s are equal and the offset voltage V_{offset} equals zero with both current and voltage bias. With a heat flux, one pair of resistors will be at temperature T_1 and the other at T_2, and the corresponding resistances can be found with

$$R_i=R_0[1+\alpha(T_i-T_0)]. \tag{8}$$

Substituting this expression for the resistances in Eq. 6 and assuming $R_3=R_1$ and $R_2=R_4$ gives the output voltage with current bias as

$$V_{out} = I\frac{R_0^2\left[1+\alpha\left(T_2-T_0\right)\right]^2 - R_0^2\left[1+\alpha\left(T_1-T_0\right)\right]^2}{2\left\{R_0\left[1+\alpha\left(T_2-T_0\right)\right]+R_0\left[1+\alpha\left(T_1-T_0\right)\right]\right\}} \tag{9}$$

With careful manipulation, Eq. 9 simplifies to

$$V_{out} = \frac{IR_0}{2}\alpha\left(T_2-T_1\right). \tag{10}$$

which shows that the output voltage for current bias is directly proportional to the resistor temperature difference or heat flux. Again, this assumes all the resistors are equal at the reference temperature T_0.

Substituting Eq. 8 for the resistances in Eq. 6 and making the same assumptions about equal resistances gives the output voltage with voltage bias as

$$V_{out} = V\frac{R_0^2\left[1+\alpha\left(T_2-T_0\right)\right]^2 - R_0^2\left[1+\alpha\left(T_1-T_0\right)\right]^2}{\left\{R_0\left[1+\alpha\left(T_2-T_0\right)\right]+R_0\left[1+\alpha\left(T_1-T_0\right)\right]\right\}^2} \tag{11}$$

which reduces to

$$V_{out} = V\frac{\alpha\left(T_2-T_1\right)}{2+\alpha\left(T_1+T_2-2T_0\right)} \tag{12}$$

With voltage bias, the output voltage is no longer a linear function of the temperature difference (T_2-T_1). In this case, the heat flux is not proportional to the output voltage, and additional measurement of either T_1 or T_2 would be necessary before the heat flux could be calculated. Thus, current biasing is a more direct determination of heat flux.

Next, consider the more realistic case (but still not the real case where all four resistors may be different) where pairs of resistors have equal values at room temperature ($R_{10}=R_{30}$ and $R_{20}=R_{40}$, but $R_{10}\neq R_{20}$) and also equal values with heat flux ($R_1=R_3$ and $R_2=R_4$). The output voltage with current bias according to Eq. 6 reduces to

$$V_{out} = I\frac{R_2^2-R_1^2}{2\left(R_2+R_1\right)} \tag{13}$$

which can be simplified to

$$V_{out} = I\frac{\left(R_2-R_1\right)}{2} \tag{14}$$

At the reference temperature, T_0, this equation becomes

$$V_{offset} = V_{out}\left(T_1=T_2=T_0\right) = \frac{I}{2}\left(R_{2_0}-R_{1_0}\right) \tag{15}$$

where V_{out} is now labeled V_{offset} since it represents the offset voltage at the reference temperature. When heat flows through the surface, one pair of resistors reach T_1 and the other T_2, the output voltage becomes

$$V_{out} = \frac{I}{2}\left\{R_{2_0}\left[1+\alpha\left(T_2-T_0\right)\right]-R_{1_0}\left[1+\alpha\left(T_1-T_0\right)\right]\right\} \tag{16}$$

which can be written as

$$V_{out} = \frac{I}{2}\left(R_{2_0}-R_{1_0}\right)-\alpha T_0\frac{I}{2}\left(R_{2_0}-R_{1_0}\right)+ \cdot$$

$$+\alpha\frac{I}{2}\left(R_{2_0}T_2-R_{1_0}T_1\right) \tag{17}$$

The first term is exactly Eq. 15 or V_{offset}; the second term is V_{offset} multiplied by αT_0. Thus, Eq. 17 can be written as

$$V_{out} = V_{offset}-\alpha T_0 V_{offset}+\alpha\frac{I}{2}\left(R_{2_0}T_2-R_{1_0}T_1\right) \tag{18}$$

Define $\Delta T = T_1 - T_2$ and $\Delta R_0 = R_{10} - R_{20}$.
The output voltage becomes

$$V_{out} = V_{offset} - \alpha T_0 V_{offset} + \alpha \frac{I}{2} R_{1_0} \Delta T \left(\frac{\Delta R_0 T_2}{R_{1_0} \Delta T} - 1 \right) \tag{19}$$

The first two terms are constants and independent of sensor temperature or heat flux. The third term contains the desired heat flux expression and an error expression which is both temperature and heat-flux dependent. To avoid having to compensate for this temperature error, it is necessary to have $\frac{\Delta R_0 T_2}{R_{1_0} \Delta T} << 1$. Under normal operating conditions, T_2 is approximately 300 K, and R_0 is approximately 300 ohms, so that the error expression can be written as $\Delta R_0 << \Delta T$. Using the sensor material properties and dimensions, along with Fourier's heat conduction law, this expression becomes $\Delta R_0[\text{ohms}] < 5q[\text{MWm}^{-2}]$ for a 10% error.

Rewriting Eq. 19 for heat flux gives

$$q = \frac{k}{d}(T_1 - T_2) = \\ = \frac{2k}{dR_{1_0} \alpha I} \left(V_{offset} - V_{offset} \alpha T_0 - V_{out} + \alpha \frac{I}{2} \Delta R \cdot T_2 \right) \tag{20}$$

This equation clearly shows that heat flux is proportional to the desired output voltage along with a temperature-dependent error term (i.e., last term in Eq. 20). This behavior can be shown more clearly by setting the heat flux equal to zero, which gives

$$V_{out} = V_{offset}(1 - \alpha T_0) + \alpha \frac{I}{2} \Delta R_0 T \tag{21}$$

which shows a linear dependence of output voltage on temperature.

The same procedure can be followed for the case of voltage biasing. In this case, the output voltage (Eq. 7) can be written as

$$V_{out} = V \frac{R_2^2 - R_1^2}{(R_2 + R_1)^2} \tag{22}$$

which can be simplified to

$$V_{out} = V \frac{R_2 - R_1}{R_1 + R_2} \tag{23}$$

At the reference temperature, T_0, the output voltage or offset voltage is

$$V_{offset} = V_{out}(T_1 = T_2 = T_0) = V \frac{R_{2_0} - R_{1_0}}{R_{1_0} + R_{2_0}} \tag{24}$$

With heat flux, the two pairs of resistors reach temperatures T_1 and T_2 and the output voltage (using Eq. 8 for R_1 and R_2) becomes

$$V_{out} = V \frac{R_2 - R_1}{R_2 + R_1} = \\ = V \frac{R_{2_0}[1 + \alpha(T_2 - T_0)] - R_{1_0}[1 + \alpha(T_1 - T_0)]}{R_{2_0}[1 + \alpha(T_2 - T_0)] + R_{1_0}[1 + \alpha(T_1 - T_0)]} = \\ = V \frac{R_{2_0} - R_{1_0} - \alpha T_0(R_{2_0} - R_{1_0}) + \alpha(R_{2_0} T_2 - R_{1_0} T_1)}{R_{2_0} + R_{1_0} + \alpha T_0(R_{2_0} - R_{1_0}) + \alpha(R_{2_0} T_2 - R_{1_0} T_1)}. \tag{25}$$

This expression can be simplified using the expressions for ΔR_0 and ΔT. Doing this gives

$$V_{out} = V \frac{\Delta R_0(1 - \alpha T_0 + \alpha T_2) - \alpha R_{1_0} \Delta T}{(2R_{1_0} + \Delta R_0)(1 - \alpha T_0 + \alpha T_2) + \alpha R_{1_0} \Delta T} \tag{26}$$

Substituting the heat-flux expression, $q = \frac{k}{d} \Delta T$, gives

$$q = \frac{k}{d} \frac{[V \Delta R_0 - V_{out}(2R_{1_0} + \Delta R_0)](1 - \alpha T_0 + \alpha T_2)}{(V_{out} + V) \alpha R_{1_0}}. \tag{27}$$

Notice, once again, there are constant terms representing the offset voltage and the reference temperature, T_0. There's also the error term which is a function of the sensor operating temperature.

Finally, consider the real case where all resistors may have different values at the reference temperature. When there is no heat flux, there is no temperature difference between resistor pairs, and $T_1=T_2=T$. For current bias, Eq. 6 becomes

$$V_{out}(T_1 = T_2 = T) =$$
$$= I\frac{\left(R_{2_0}R_{4_0} - R_{1_0}R_{3_0}\right)[1+\alpha(T-T_0)]^2}{\left(R_{1_0}+R_{2_0}+R_{3_0}+R_{4_0}\right)[1+\alpha(T-T_0)]} =$$
$$= I\frac{\left(R_{2_0}R_{4_0} - R_{1_0}R_{3_0}\right)}{\left(R_{1_0}+R_{2_0}+R_{3_0}+R_{4_0}\right)}[1+\alpha(T-T_0)] =$$
$$= V_{offset}[1+\alpha(T-T_0)].$$

(28)

The offset voltage is zero if $R_{20}R_{40}$ equals $R_{10}R_{30}$. If not, the output voltage has a linear dependence on temperature. The zero-heat-flux case for voltage bias from Eq. 7 becomes

$$V_{out}(T_1 = T_2 = T) =$$
$$= V\frac{\left(R_{2_0}R_{4_0} - R_{1_0}R_{3_0}\right)[1+\alpha(T-T_0)]^2}{\left(R_{1_0}+R_{2_0}\right)\left(R_{3_0}+R_{4_0}\right)[1+\alpha(T-T_0)]^2} =$$
$$= V\frac{\left(R_{2_0}R_{4_0} - R_{1_0}R_{3_0}\right)}{\left(R_{1_0}+R_{2_0}\right)\left(R_{3_0}+R_{4_0}\right)} = V_{offset}.$$

(29)

In this case, the output voltage is independent of sensor temperature. This is one advantage to voltage biasing.

Now consider the simplified, two-resistor sensor.

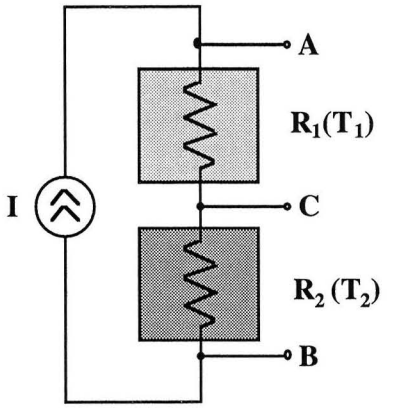

As shown in the figure, when the two resistors are connected in series, the voltage across each of the sensors can be measured and combined as

$$V_{out} = V_{CB} - V_{AC} \tag{30}$$

With zero heat flux, $T_1 = T_2$ and the output voltage equals

$$V_{out}(T_1 = T_2 = T_0) = V_{offset} = I\left(R_{2_0} - R_{1_0}\right). \tag{31}$$

With heat flux, the temperatures are different and the output voltage becomes

$$V_{out} = I\left\{R_{2_0}\left[1+\alpha(T_2-T_0)\right] - R_{1_0}\left[1+\alpha(T_1-T_0)\right]\right\} =$$
$$= I\left(R_{2_0}-R_{1_0}\right) + \alpha T_0 I\left(R_{2_0}-R_{1_0}\right) + \alpha I\left(R_{2_0}T_2 - R_{1_0}T_1\right) =$$
$$= V_{offset} - \alpha T_0 V_{offset} + \alpha I\left(R_{2_0}T_2 - R_{1_0}T_1\right). \tag{32}$$

which can be written as

$$V_{out} = V_{offset} - \alpha T_0 V_{offset} + \alpha I\left(R_{2_0}T_2 - R_{1_0}T_1\right) =$$
$$= V_{offset} - \alpha T_0 V_{offset} + \alpha I R_{1_0}\Delta T\left(\frac{T_2\Delta R}{\Delta T R_{1_0}} - 1\right). \tag{33}$$

This is the same form as Eq. 19 for the Wheatstone bridge under constant current biasing. Once again, the output voltage has a linear dependence on temperature. The alternative is to consider a weighted output voltage difference according to

$$\frac{V_{CB}}{R_{2_0}} - \frac{V_{AC}}{R_{1_0}} = \frac{IR_2}{R_{2_0}} - \frac{IR_1}{R_{1_0}} =$$

$$= \frac{IR_{2_0}\left[1+\alpha(T_2 - T_0)\right]}{R_{2_0}} - \frac{IR_{1_0}\left[1+\alpha(T_1 - T_0)\right]}{R_{1_0}} =$$

$$= I\alpha(T_2 - T_1). \tag{34}$$

The heat flux can be expressed as

$$q = \frac{k}{d}(T_2 - T_1) = \frac{k}{d}\frac{1}{\alpha I}\left(\frac{V_{CB}}{R_{2_0}} - \frac{V_{AC}}{R_{1_0}}\right) \tag{35}$$

In this case, the heat flux is proportional to the weighted voltage difference and independent of sensor temperature. This requires accurate measurement of the two resistances at the reference temperature. These considerations show that heat flux measurements using resistive thermometers require either resistor trimming to balance the gauge or signal conditioning to compensate for an unbalanced gauge.

Conclusions

Using a plug-type reference sensor, the unamplified thin-film sensor's steady-state sensitivity was found to be 1 mV/MWm^{-2}. A frequency response curve, up to 8 kHz, was also determined. This curve was compared to that obtained with a 1-D finite-element model. Equations for a Wheatstone bridge and a two-resistor sensor were derived for both voltage and current biasing. An expression for the resistor tolerance for an error less than 10% at any given heat flux was found.

Acknowledgments

This work was supported by the Army Research Office, Multidisciplinary University Research Initiative contract # DAAH04-95-10097. The authors want to thank C. A. Bang and B. J. Boggs from Advanced MicroMachines Incorporated, Cleveland, Ohio, for providing the sensors and test equipment, and for technical discussions.

References

[1] Epstein, A.H., Guenette, G.R., et al., "High-Frequency Response Heat-Flux Gauge," Review of Scientific Instruments, Vol. 57, pp 639-649, April 1986.

[2] Hager, J.M., Simmons, S., et al., "Experimental Performance of a Heat-Flux Microsensor," Journal of Engineering for Gas Turbines and Power, Vol. 113, pp 246-250, April 1991.

[3] Godefroy, J.C., Clery, M., et al., "Thin Film Temperature Heat Fluxmeters," J. Thin Solid Films, Vol. 193/194, pp 924-934, 1990.

[4] Bhatt, H. and Fralick, G., "Novel Thin-Film Heat Flux Sensors: Fabrication and Calibration," AIAA 4th Int. Aerospace Plane Conf., December 1992, Orlando, FL.

[5] Cho, C.S.K and Fralick, G.C., "Measurement of Frequency Response and Steady State Response of a Novel Thin Film Heat Flux Gage," 31st AIAA/ASME/SAE/ASEE Joint Propulsion Conference and Exhibit, July 1995, San Diego, CA.

[6] Liebert, C.H., "Miniature Convection Cooled Plug-Type Heat Flux Gauges," 40th International Instrumentation Symposium, Instrument Society of America, May 1994, Baltimore, MD.

[7] Mehregany, M. and Bang, C.A., "MEMS for Smart Structures," in Proceedings of SPIE Smart Structures and Materials Conference, Feb. 1995, San Diego, CA.

[8] Hager, J.M., Onishi, S., et. al., "Heat Flux Microsensors," Heat Transfer Measurements, Analysis and Flow Visualization, R.K. Shah, ed., ASME, pp. 1-8, 1989.

REPORT DOCUMENTATION PAGE

Form Approved
OMB No. 0704-0188

1. AGENCY USE ONLY (*Leave blank*)	2. REPORT DATE	3. REPORT TYPE AND DATES COVERED
	April 1998	Technical Memorandum

4. TITLE AND SUBTITLE

Experimental Performance of a Micromachined Heat Flux Sensor

5. FUNDING NUMBERS

WU–523–21–13–00
1L161102AH45

6. AUTHOR(S)

S. Stefanescu, R.G. DeAnna, and M. Mehregany

7. PERFORMING ORGANIZATION NAME(S) AND ADDRESS(ES)

NASA Lewis Research Center
Cleveland, Ohio 44135–3191
and
U.S. Army Research Laboratory
Cleveland, Ohio 44135–3191

8. PERFORMING ORGANIZATION REPORT NUMBER

E–10821

9. SPONSORING/MONITORING AGENCY NAME(S) AND ADDRESS(ES)

National Aeronautics and Space Administration
Washington, DC 20546–0001
and
U.S. Army Research Laboratory
Adelphi, Maryland 20783–1145

10. SPONSORING/MONITORING AGENCY REPORT NUMBER

NASA TM–107517
ARL–MR–363

11. SUPPLEMENTARY NOTES

Prepared for the Joint Propulsion Conference cosponsored by AIAA, ASME, SAE, and ASEE, Seattle, Washington, July 6–9, 1997. S. Stefanescu and M. Mehregany, Case Western Reserve University, Cleveland, Ohio 44106; R.G. DeAnna, U.S. Army Research Laboratory, NASA Lewis Research Center. Responsible person, R.G. DeAnna, organization code 5510, (216) 433–3385.

12a. DISTRIBUTION/AVAILABILITY STATEMENT

Unclassified - Unlimited
Subject Categories: 34 and 35 *Distribution:* Nonstandard

This publication is available from the NASA Center for AeroSpace Information, (301) 621–0390.

12b. DISTRIBUTION CODE

13. ABSTRACT ***(Maximum 200 words)***

Steady-state and frequency response calibration of a microfabricated heat-flux sensor have been completed. This sensor is batch fabricated using standard, micromachining techniques, allowing both miniaturization and the ability to create arrays of sensors and their corresponding interconnects. Both high-frequency and spatial response is desired, so the sensors are both thin and of small cross-sectional area. Thin-film, temperature-sensitive resistors are used as the active gauge elements. Two sensor configurations are investigated: a Wheatstone-bridge using four resistors; and a simple, two-resistor design. In each design, one resistor (or pair) is covered by a thin layer (5000 Å) thermal barrier; the other resistor (or pair) is covered by a thick (5 μm) thermal barrier. The active area of a single resistor is 360 μm by 360 μm; the total gauge area is 1.5 mm square. The resistors are made of 2000 Å-thick metal; and the entire gauge is fabricated on a 25 μm-thick flexible, polyimide substrate. Heat flux through the surface changes the temperature of the resistors and produces a corresponding change in resistance. Sensors were calibrated using two radiation heat sources: a furnace for steady-state, and a light and chopper for frequency response.

14. SUBJECT TERMS

Heat-flux sensor; Thin film; Microfabricated

15. NUMBER OF PAGES

17

16. PRICE CODE

A03

17. SECURITY CLASSIFICATION OF REPORT	18. SECURITY CLASSIFICATION OF THIS PAGE	19. SECURITY CLASSIFICATION OF ABSTRACT	20. LIMITATION OF ABSTRACT
Unclassified	Unclassified	Unclassified	